Hindawi
Mathematical Problems in Engineering
Volume 2021, Article ID 2583707, 11 pages
https://doi.org/10.1155/2021/2583707

Research Article

Investigation on Rock Strata Fracture Regulation and Rock Burst Prevention in Junde Coal Mine

Fengnian Wang,[1,2] **Gan Li**,[2,3] **and Chi Liu**[4]

[1]*State Key Laboratory for Geomechanics and Deep Underground Engineering, China University of Mining and Technology (Beijing), Beijing 100083, China*
[2]*School of Mechanics and Civil Engineering, China University of Mining and Technology (Beijing), Beijing 100083, China*
[3]*Ningbo University, Ningbo 315000, China*
[4]*State Key Laboratory of Hydroscience and Engineering, Tsinghua University, Beijing 100084, China*

Correspondence should be addressed to Gan Li; ligan303@126.com

Received 28 August 2021; Accepted 12 September 2021; Published 26 September 2021

Academic Editor: Feng Xiong

Through the establishment of structural mechanics model, this paper analyzes the fracture of super thick rock stratum. Through the model, it can be seen that the fracture of low-level super thick rock stratum produces large elastic energy release and dynamic load, which is easy to produce disasters such as rock burst. The numerical calculation shows that under the influence of low hard and thick rock stratum, the leading area of coal mine roadway will produce energy concentration, and the coal pillar will also produce energy accumulation. Thick rock stratum is in bending state and has large bending elasticity. Coal pillar has large compression elasticity, which is the main reason for rock burst. The accumulation of elastic properties of overburden and rock burst caused by coal pillar energy storage can be effectively controlled by using advanced presplitting blasting, coal seam drilling pressure relief, and strengthening support.

1. Introduction

In China, the geological conditions of coal mine are complex, and the underground mining is gradually developed from shallow to deep. In recent years, in the process of coal mining, rock burst caused by many factors, such as improper mining design, coal pillar setting, unknown geological conditions, and high in situ stress, has caused huge casualties and property losses. The rock burst disaster in engineering practice has challenged the existing accident mechanism research, treatment scheme, and prediction theory. Many experts have done a lot of research, e.g., Guo et al. [1] studied the mechanical properties and fracture process characteristics of deep buried granite specimens under different initial confining pressure and unloading rate combinations. Based on the analysis of the causes of dynamic disasters, Liang et al. [2] proposed a reasonable filling height of goaf under special geological conditions in order to fully eliminate mine disasters. Jiao et al. [3] analyzed the correlation between fault structure and temporal and spatial characteristics of rock burst by collecting rock burst events occurred near fault in the process of deep mining. He et al. [4, 5] developed the key technologies such as roof directional presplitting technology, negative Poisson's ratio high prestressed constant resistance support technology, and coal gangue plugging support technology, which are conducive to reducing the stress concentration of coal pillar and rock burst accidents. Ning et al. [6] put forward and applied the soft and strong support body as the support form of gob side entry retaining. In the early stage of roof movement, the soft strong support has good compressibility, which can not only relieve the roof pressure and strong impact load but also reduce the support resistance and prevent the support from being crushed. Zhu et al. [7] analyzed and evaluated the risk of rock burst, considering the coupling behavior of stress distribution and overlying strata movement. Based on the principle of strain

energy balance, the height of pressure relief zone above the goaf of an underground mining area is determined for the first time. Kong et al. [8] studied the deformation and rock burst risk of roadway under different dynamic and static loads. Dou et al. [9] systematically studied the relationship between elastic wave velocity and coal sample stress and put forward the positive correlation between elastic wave velocity and stress under uniaxial compression. Wang et al. [10, 11] analyzed the distribution characteristics of stress field under gob side entry retaining with roof cutting. Wang et al. [12] studied the failure mechanism of marble under cyclic loading and unloading conditions and provided theoretical basis for rock dynamic disaster prediction. With the development of mining activities, the self-stable state of high stress balance of coal pillar is easily broken by the impact energy formed by the sudden collapse of key strata [13, 14]. Therefore, the rock burst of coal pillar in overlying coal area is the result of static load and dynamic load [15, 16]. At present, the more effective control methods of rock burst mainly include pressure relief, support reinforcement, presplitting roof, and eliminating coal pillar [17, 18].

Through theoretical analysis, numerical calculation, and field engineering practice, this paper analyzes the occurrence mechanism and control measures of rock burst from the perspective of energy distribution. The characteristics of advance and lateral energy distribution of roadway under low-level and thick rock stratum are put forward. The strategy of controlling rock burst by means of advanced presplitting is put forward.

2. Engineering Geological Conditions

Junde minefield is located in the southern end of Hegang coalfield. The fold of the minefield is simple. The coal measure strata is a NNE trending, east dipping monoclinic structure, with local undulate. There are 128 faults in the minefield. Most of them are tension and torsion normal faults. Among them, 62 faults have a drop of more than 30 m, 27 faults have a drop of 15–30 m, and the rest of the faults have a drop of less than 15 m. Most of them are in direct contact with the quaternary system.

9103 working face adopts strike longwall comprehensive mechanized mining method. The strike of the working face is 1637 m, the average length of the working face is 168 m, and the mining height is 3.6 m. The occurrence of coal seam in the working face is stable, mainly massive and small bright coal, a small amount of dark coal, and the coal quality is good. The thickness of the coal seam is 8.21–14.15 m, with an average thickness of 11.18 m. The coal seam is mined in layers, and the recoverable reserves are 4.304 million tons. According to the drilling data and roadway observation, the pseudoroof of the coal seam is 0.2–3.33 m carbon shale, the direct roof of the coal seam is 5.2–14.9 m gray siltstone, and the main roof is coarse sandstone, and there is conglomerate locally. The roof condition is shown in Figure 1.

The results of in situ stress measurement show that the maximum principal stress is approximately in horizontal direction, near east-west direction, which is unfavorable to the north-south direction of roadway support. In this area, the maximum principal stress ranges from 22.8 MPa to 27.3 MPa, near east-west direction; minimum principal stress range is 10.1–12.8 MPa, near vertical direction. At present, the conveyor roadway and return air roadway are arranged in the north-south direction, which is approximately vertical to the maximum principal stress, and the roadway is prone to large deformation, which is not conducive to the maintenance of the roadway.

After mining, the original stress field will redistribute, and the coal and rock will have different degrees of damage and movement. The overlying strata affected by mining include the strata that participate in the movement along the advancing direction and the strata that participate in the movement along the working face direction. The stress field is divided into abutment pressure distribution in front of working face and lateral stress field. When the support pressure is too large, the accumulated elastic energy of coal is greater than its bearing capacity, which will lead to failure and even rock burst. At the same time, because of the high strength and thickness of the roof, the release of elastic energy during breaking is easy to produce rock burst [19, 20].

As shown in Figure 2, it shows the movement diagram of overlying strata in the direction of coal seam advancement. When the strata fall behind and the weight of the overlying strata is transferred to the front of the working face, the peak of support pressure will eventually appear, which is easy to lead to rock burst. At the same time, the overlying strata fracture will release the accumulated bending elastic energy of the rock beam, resulting in energy transfer and rock burst.

The calculation of the first fracture weighting step of the thick rock beam is shown in formula (1), and the periodic weighting step is shown in the following formula:

$$v_\varepsilon = \int_{t_0}^{t_1} \sigma : \delta\varepsilon = \int_0^1 t\sigma : (t\delta\varepsilon) = \sigma : \varepsilon \int_0^1 t\delta t = \frac{1}{2}\sigma : \varepsilon = \frac{1}{2}\sigma_{ij}\varepsilon_{ij}, \tag{1}$$

$$C_i = -\frac{1}{2}C_{i-1} + \frac{1}{2}\sqrt{C_{i-1}^2 + \frac{4M_s^2[\sigma_s]}{3\gamma(M_s + M_c)}}, \tag{2}$$

where M_S, M_C are the thickness of the lower (supporting) strata and the upper (following) strata of the rock beam, m; σ_S is the allowable tensile stress of lower (supporting) rock stratum, MPa; r is the average unit weight of rock mass, kg/$m3 \times 103$; C_i, $C_{i\text{-}1}$ are the weighting step of the same period and the weighting step of the last period, m.

There is a strong correlation between the overlying strata movement along the working face direction and the working face length. The longer the working face length is [21, 22], the higher the development height of the fracture arch is. The shorter the length of working face is, the smaller the development height of fracture arch is. However, under the influence of low-level thick rock, the development of fracture arch height has a strong correlation with the position of thick rock, and its development process is different from that of common fracture arch.

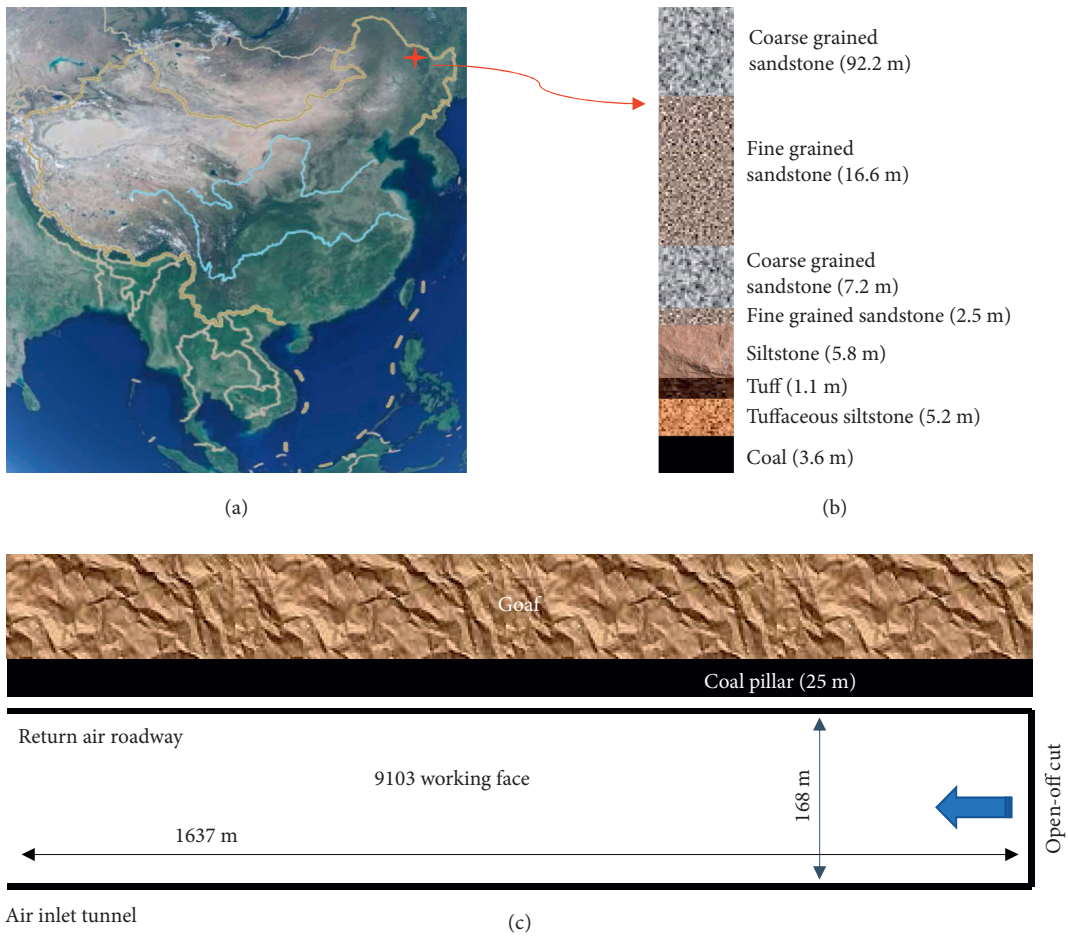

Figure 1: Location and overview of the study target structural mechanics model and disaster mechanism of coal seam mining under low position and extremely thick strata (map source: official website of the Ministry of Natural Resources of China).

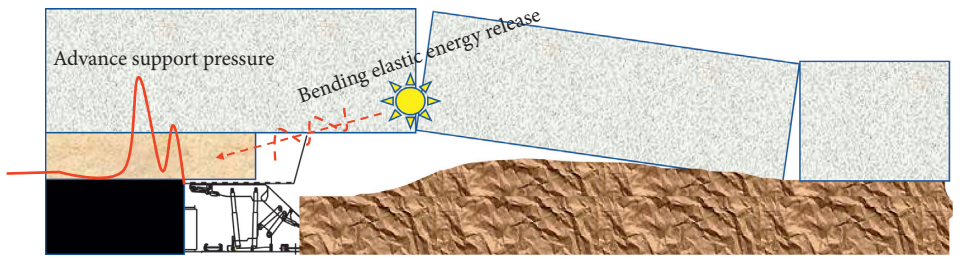

Figure 2: Fracture model of overlying strata.

According to the analysis in Figure 3, the height of the fracture arch is always below the low position thick rock beam before the low position thick rock beam is broken. In the strike long arm mining method, with coal pillar roadway protection, the weight of low position thick rock beam is shared by the embedded end of rock beam and coal pillar. When the embedded part of the thick rock beam cracked, the weight of the low thick rock beam was transferred from the fracture line of the rock beam to the coal pillar. Before the fracture, the overhanging roof of the low position thick rock beam is large, and it has high-strength bending elastic energy and gravitational potential energy.

3. Numerical Calculation Model and Results

3.1. Numerical Calculation Model and Its Parameters. According to the comprehensive histogram of 9103 working face in Junde Coal Mine, the initial three-dimensional numerical model is established with the help of 3DEC numerical simulation analysis software, as shown in Figure 4. The model is 2000 m long, 500 m wide, and 450 m high. Mohr–Coulomb model is adopted as the constitutive model of the numerical model. The selection of rock mechanics parameters in the model is determined based on the rock mechanical parameters obtained in the

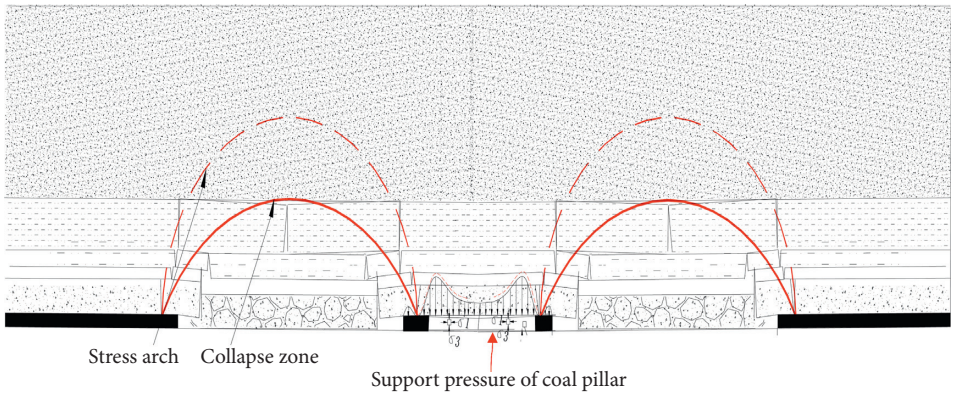

Figure 3: Lateral support pressure of stope.

laboratory and the inversion based on the field measured data, as shown in Table 1. The bottom boundary of the model is fully constrained in X, Y, and Z directions, and the top is free.

According to the identification of the impact tendency of 17 layers in Junde Coal Mine, the following conclusions can be drawn: the average failure time of coal sample is 485.2 ms, the average impact energy index is 4.108, the average elastic energy index is 2.531, and the uniaxial compressive strength is 15.176 MPa, which belongs to weak impact tendency; the tensile strength of the rock sample is 1.8 MPa, the thickness of the roof is 14.4 m, the elastic modulus is 95.5 GPa, the load per unit width of the overlying strata is 0.0378 MPa, and the bending energy index is 821.928, which is strongly impact-prone.

3.2. Strata Movement Law and Energy Response in Strike Mining Direction. According to the strength theory, if the local stress of coal and rock mass is too large and exceeds its own strength, rock burst will be induced. According to energy theory, rock burst will be induced when the energy of mechanical system of stope surrounding rock exceeds the energy needed to maintain the equilibrium state [23, 24].

For linearly elastic materials, the strain energy density is shown in the following equation:

For an isotropic linear elastic material, the strain energy density is

$$v_\varepsilon(\varepsilon) = \frac{1}{2}\sigma : \varepsilon = \mu\varepsilon : \varepsilon + \frac{1}{2}\lambda tr^2(\varepsilon) = \mu tr(\varepsilon : \varepsilon) + \frac{1}{2}\lambda tr^2(\varepsilon). \tag{3}$$

The strain energy density can also be given by the three principal strains (eigenvalues) of the strain tensor.

$$v_\varepsilon(\varepsilon_1, \varepsilon_2, \varepsilon_3) = \mu\left(\varepsilon_1^2 + \varepsilon_2^2 + \varepsilon_3^2\right) + \frac{1}{2}\lambda(\varepsilon_1 + \varepsilon_2 + \varepsilon_3)^2. \tag{4}$$

Using the principal stress expression form,

$$v_\varepsilon(\sigma_1, \sigma_2, \sigma_3) = \frac{1+\nu}{2E}\left(\sigma_1^2 + \sigma_2^2 + \sigma_3^2\right) - \frac{\nu}{2E}(\sigma_1 + \sigma_2 + \sigma_3)^2. \tag{5}$$

When the model excavation is 75 m, the peak area of abutment pressure is about 2 m in front of the working face, the highest value is about 43 MPa, and the influence range of advance abutment pressure is about 50 m. The upper thick rock is not fractured, and the change of elastic energy caused by mining is about 50 m in front of the working face. The maximum energy accumulation is 4e10 J, as shown in Figure 5.

When the model is excavated for 175 m, the huge thick rock is fractured, the peak area of abutment pressure is about 5 m in front of the working face, the highest value is about 36.7 MPa, and the influence range of advance abutment pressure is about 125 m. The change of elastic energy caused by mining is in the range of about 125 m in front of the working face, as shown in Figure 6.

3.3. Distribution Characteristics of Lateral Stress. Different mining parameters (mainly referring to the length of working face) lead to different overlying strata movement and lateral stress distribution. According to the theoretical analysis and field observation, we know that the influence range of lateral abutment pressure caused by overlying huge thick strata is large, and the stress concentration factor is high, especially when the coal pillar is reserved, the elastic energy accumulated on the coal pillar is very dangerous.

As shown in Figure 7, according to the simulation, when the working face length is 145 m, the fracture arch stops when it develops to the bottom of the thick rock, but the thick rock has slight bending deformation. The influence range of front abutment pressure is 0–180 m, and the peak area of abutment stress is about 25 m. When the length of the second working face is 150 m, 25 m coal pillar is reserved, and the fracture arch stops when it develops to the bottom of the thick rock, but cracks appear in the thick rock, and there is a large bending deformation. The deformation of coal pillar is large, and the gathering elastic energy is large, so it is easy to produce rock burst.

When the length of the working face is 298 m, the huge thick strata fracture, the influence range of lateral support is 0–190 m, the peak area of support pressure is about 18 m, and the range of internal stress field is about 0–5 m.

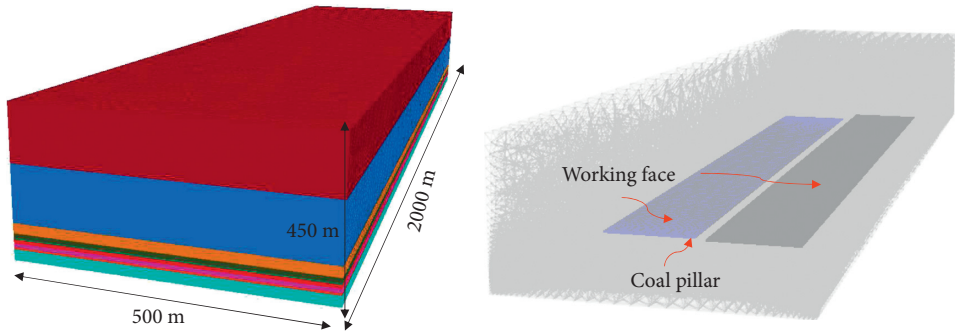

Figure 4: Numerical calculation model.

Table 1: Rock mechanics parameters.

Lithology	Compressive strength (R/MPa)	Elastic modulus (E/MPa)	Poisson's ratio	Cohesion (C/MPa)	Internal friction angle	Density
Coarse sandstone	10.934	1413.5275	0.2618	1.6863	20.02	1.8172
Medium sandstone	7.777	1030.5988	0.231	1.5554	20.02	1.7171
Fine sandstone	9.471	1346.3219	0.2156	1.8711	20.79	1.7402
Siltstone	9.394	1211.5411	0.231	1.9789	20.79	1.7094
Tuff	8.296	1069.9324	0.204	1.7476	18.36	1.5096

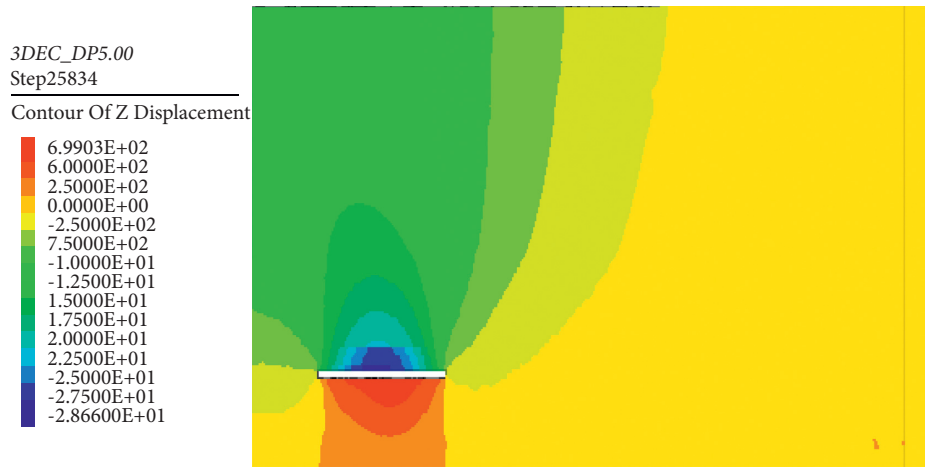

(a)

Figure 5: Continued.

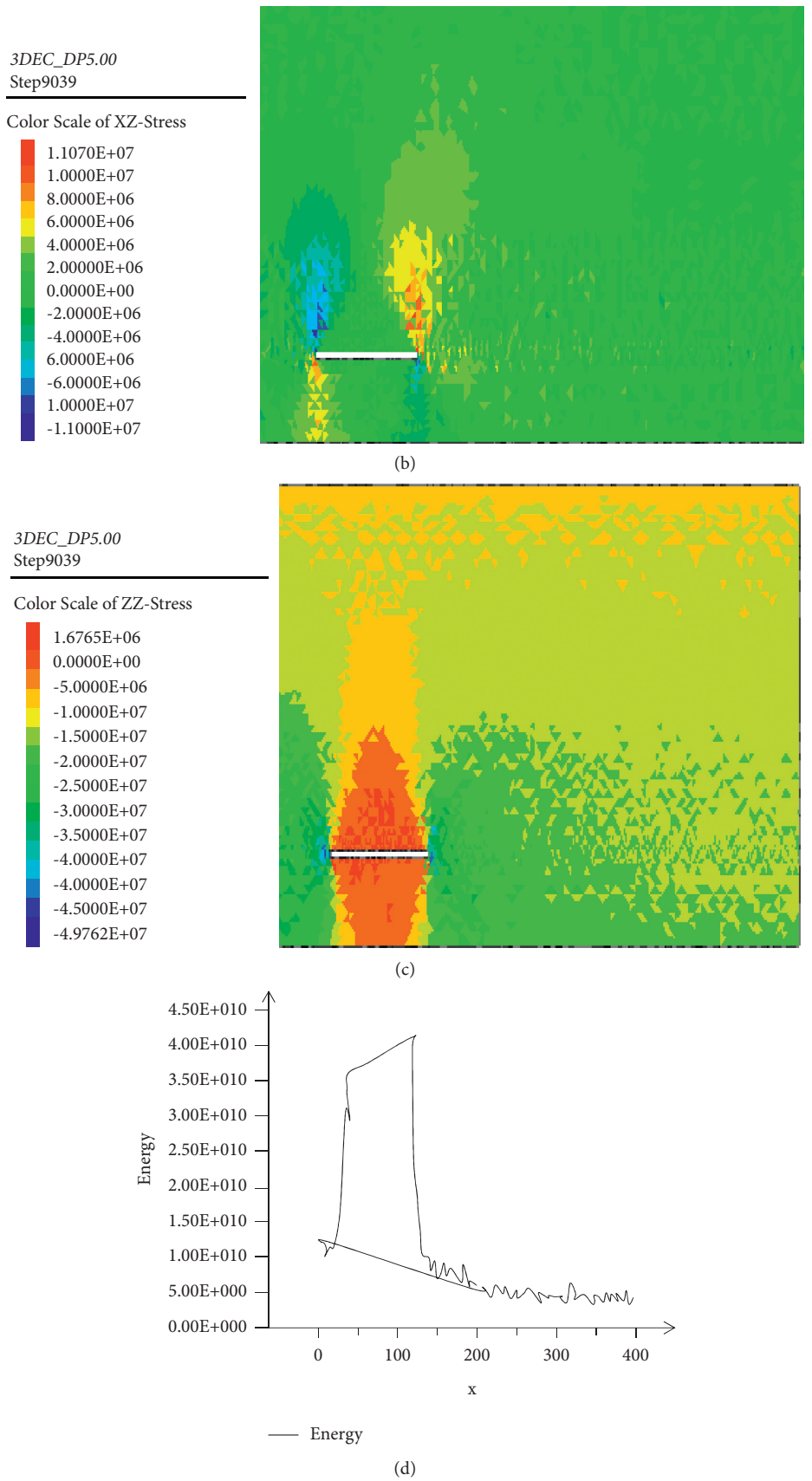

Figure 5: Distribution of displacement, stress, and energy under the condition of 75 m strike advance. (a) Displacement characteristics, (b) shear stress, (c) vertical stress, and (d) energy distribution characteristics.

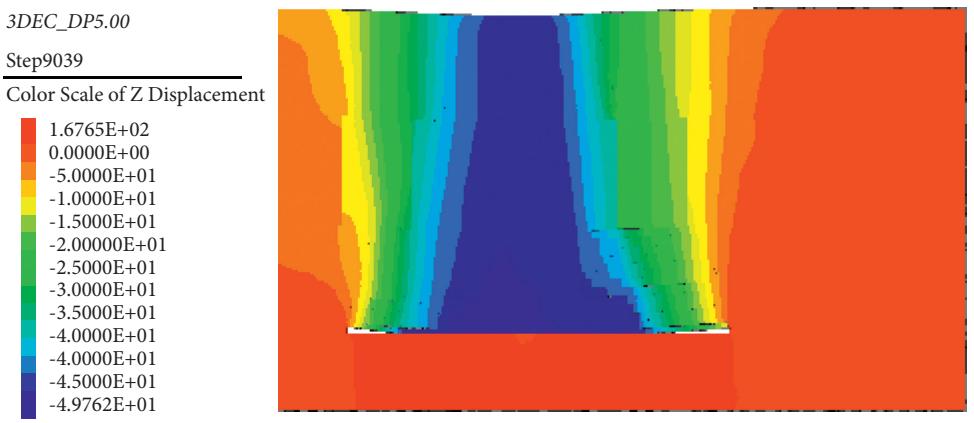

(a)

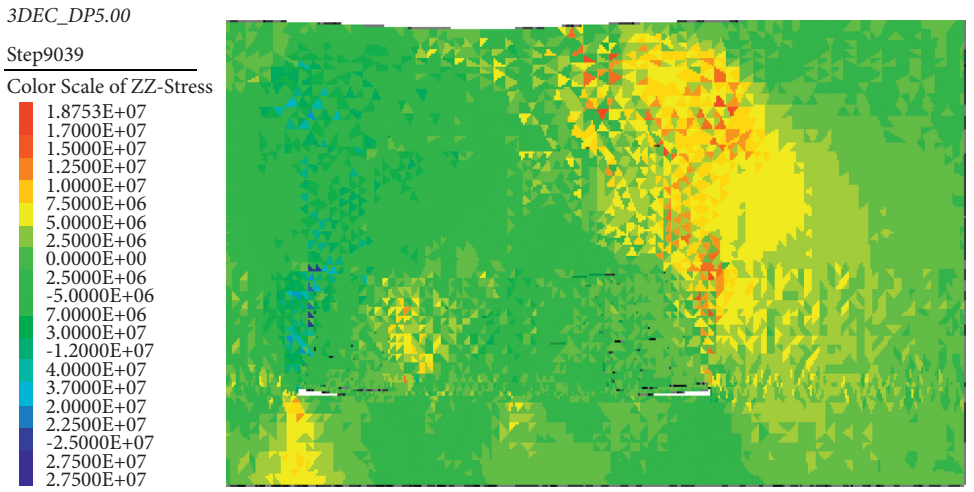

(b)

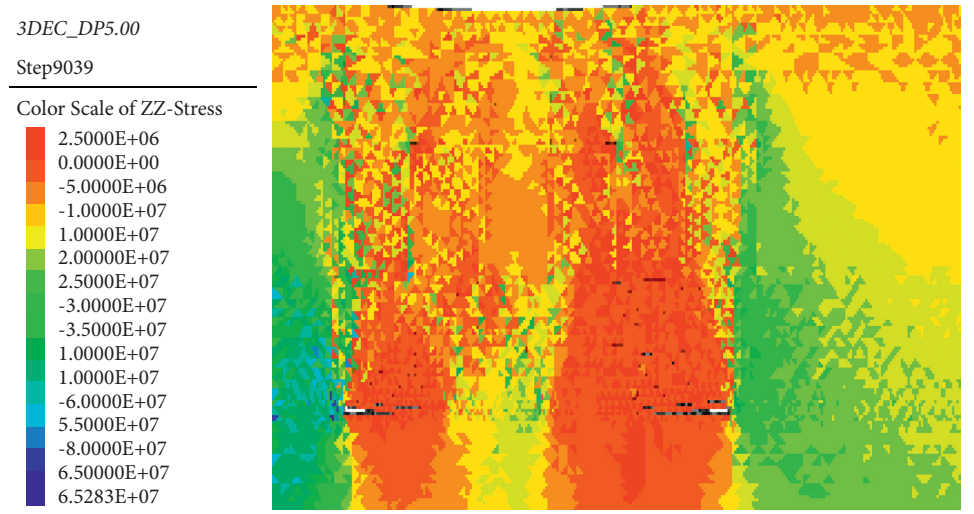

(c)

Figure 6: Continued.

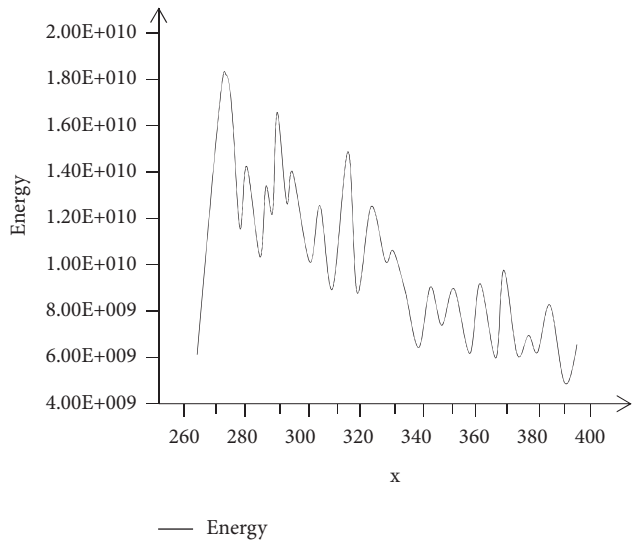

(d)

Figure 6: Distribution of displacement, stress and energy under 175 m strike advance. (a) Displacement characteristics, (b) stress, (c) vertical stress, and (d) energy distribution characteristics.

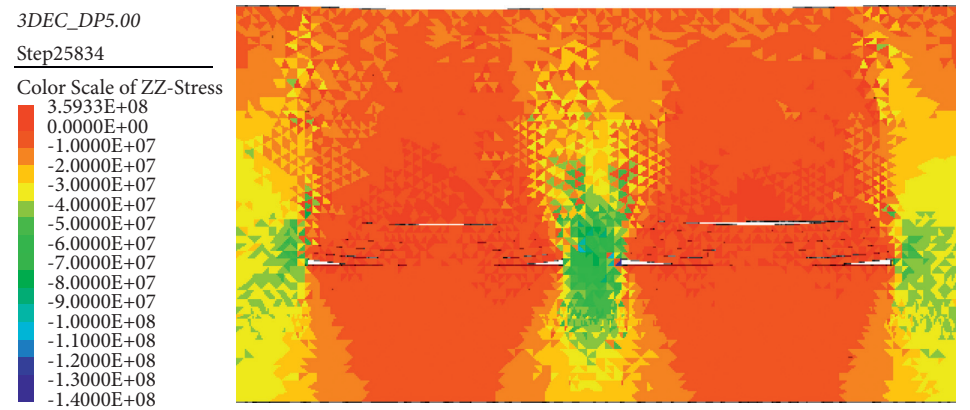

(a)

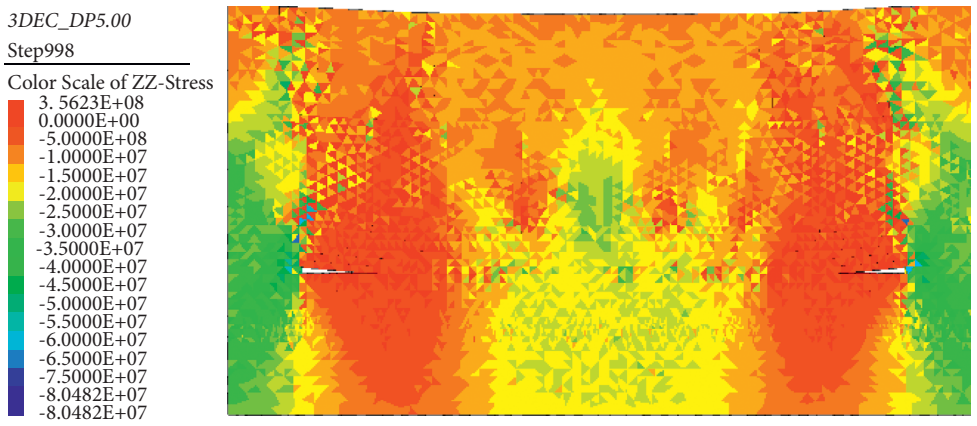

(b)

Figure 7: Stope stress characteristics under different working face lengths. (a) Cloud chart of lateral stress when working face length is 150 m. (b) Cloud chart of lateral stress when working face length is 298 m.

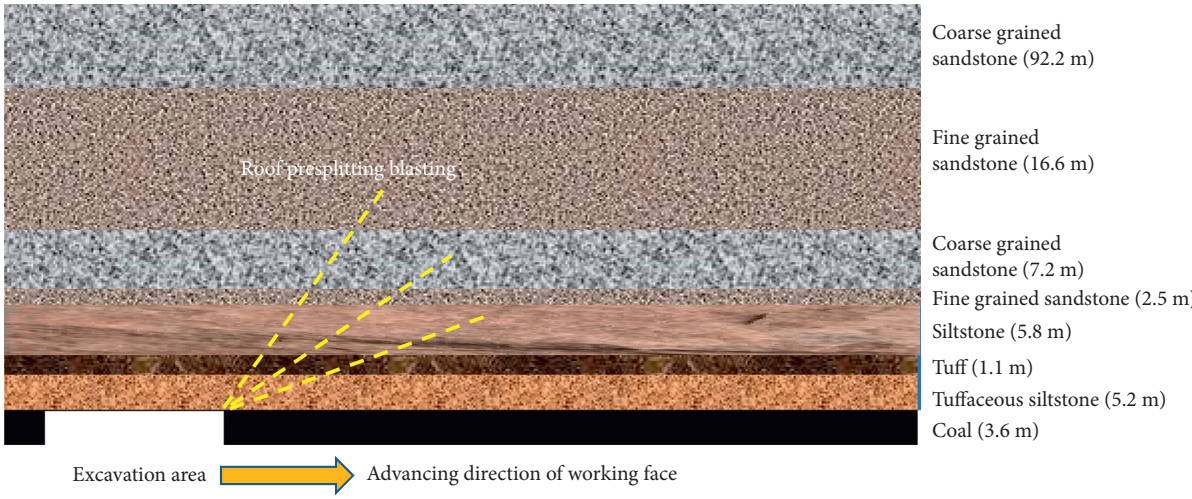

Figure 8: Advance presplitting blasting.

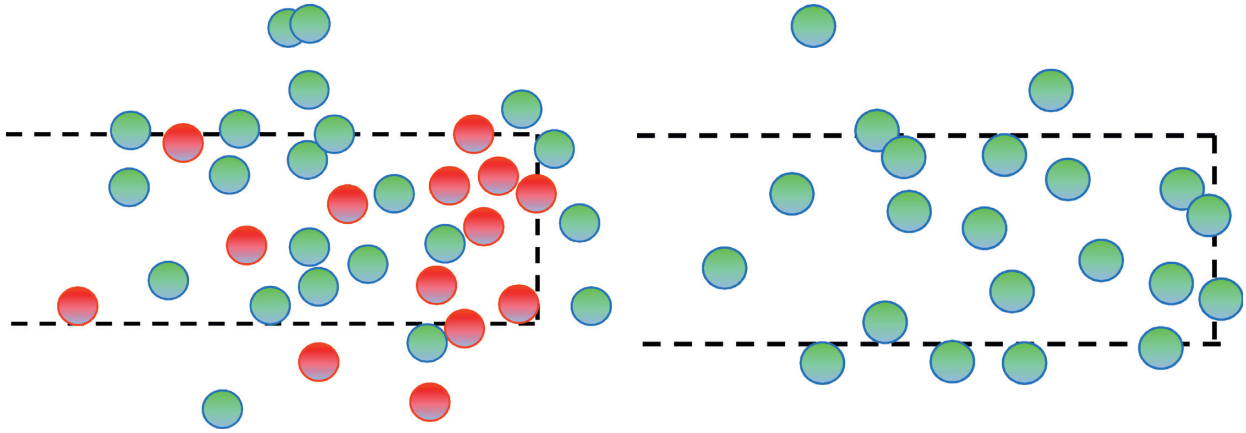

Figure 9: Influence of comprehensive treatment measures on microseism of working face, (a) in working face without comprehensive treatment, and (b) microseism of working face after comprehensive treatment.

According to theoretical analysis, field measurement, and numerical simulation, it should be determined that the length of working face is greater than 298 m, and after the rock strata collapse and stress redistribution of the previous working face is stable, gob side entry retaining or gob side entry driving should be carried out in the internal stress field, so as to avoid rock burst caused by elastic energy accumulation of overlying strata and energy stored in coal pillar of the previous working face.

4. Control Measures

In order to reduce the accumulation of elastic properties, three methods are mainly used: advance presplitting blasting, coal seam drilling pressure relief, and strengthening support. As shown in Figure 8, three boreholes are constructed in each group for roof presplitting blasting, with elevation angles of 6°, 23°, and 40° and hole length of 80 m and hole spacing of 20 m. By strengthening the support, the excessive expansion of the loose zone is limited to reduce the convergence deformation of the surrounding rock of the roadway and enhance the antiexpansion and anti-impact ability of the surrounding rock. The support section is supported by 4 anchor cables, 3 anchor bolts, and combined W-type steel belt.

Figure 9 shows the difference of microseismic distribution between two adjacent working faces before and after adopting control measures. The red sphere indicates that the microseismic energy is greater than 10e6 J, and the green sphere indicates that the energy is between 10e5 J and 10e6 J. After adopting comprehensive measures, the phenomenon of microseismic energy greater than 10e6 J disappears in the mining process. The overall number of microseisms also decreased. After the treatment, there is no big rock burst phenomenon in the mining face.

5. Conclusion

This paper expounds the dynamic basis of rock burst, analyzes the influence of overburden movement on rock burst,

and verifies it by theoretical calculation and numerical simulation.

(1) The causes of rock burst accidents in the process of excavation are as follows: the upper working face is short, the thick rock stratum is in bending state, the greater bending elastic property is accumulated, the greater compression elastic property is accumulated in the coal pillar, the width of the reserved coal pillar exceeds the "range of internal stress field", and the roadway is located in the peak area of abutment pressure. There are many risks of rock burst in the roadway maintained in the peak area of abutment pressure.

(2) The causes of rock burst accidents in the process of mining are as follows: the length of the working face in the upper section is short, the movement of the main roof (especially the extremely thick rock) is not sufficient, resulting in the storage of high-strength bending elastic energy, the wide isolation coal pillar, resulting in a large area of suspended roof, the accumulation of high-strength compression elastic energy and bending elastic performance of the roof, the fracture of the extremely thick rock in the roof, and the compression of the coal wall. It results in the release of large area roof bending elastic energy and coal wall compression elastic property.

(3) According to the experiment, it is known that when the working face is advanced to 235 m or so, the huge thick strata fracture occurs. With the advance of the working face, the abutment pressure transfers to the front of the coal wall, and its influence range gradually increases with the advance of the working face, and the leading influence distance is about 50 m. When the length of the working face is 298 m, the huge thick strata fracture occurs, the influence range of lateral support is 0–190 m, the peak area of support pressure is about 18 m, and the range of internal stress field is about 0–5 m.

(4) Advance presplitting blasting, coal seam drilling pressure relief, and strengthening support can effectively control the overburden aggregation performance and rock burst caused by coal pillar energy storage.

Data Availability

The data are available and explained in this article; readers can access the data supporting the conclusions of this study.

Conflicts of Interest

The authors declare no conflicts of interest.

Acknowledgments

This work was supported by the National Key Research and Development Plan (No. 2018YFC1504902) and the National Natural Science Foundation of China (41941018).

References

[1] J. Guo, P. Liu, J. Fan, X. Shi, and X. Huang, "Influence of confining pressure unloading rate on the strength characteristics and fracture process of granite using lab tests," *Advances in Materials Science and Engineering*, vol. 2021, no. 10, 16 pages, Article ID 7925608, 2021.

[2] W. Liang, Y. P. Cheng, and C. Xu, "The controlling effect of thick-hard igneous rock on pressure relief gas drainage and dynamic disasters in outburst coal seams," *Natural Hazards*, vol. 66, no. 2, pp. 1221–1241, 2013.

[3] Z. Jiao, Q. Yuan, P. Zou, and B. Shi, "Case study of the characteristics and mechanism of rock burst near fault in yima coalfield, China," *Shock and Vibration*, vol. 2021, no. 11, 12 pages, Article ID 9950273, 2021.

[4] M. He, Q. Wang, and Q. Wu, "Innovation and future of mining rock mechanics," *Journal of Rock Mechanics and Geotechnical Engineering*, vol. 13, no. 1, 21 pages, 2021.

[5] C. Zhu, M. C. He, M. Karakus, X. H. Zhang, and Z. Guo, "The collision experiment between rolling stones of different shapes and protective cushion in open-pit mines," *Journal of Mountain Science*, vol. 18, no. 5, pp. 1391–1403, 2021.

[6] J. Ning, J. Wang, X. Liu, K. Qian, and B. Sun, "Soft-strong supporting mechanism of gob-side entry retaining in deep coal seams threatened by rockburst," *International Journal of Mining Science and Technology*, vol. 24, no. 6, pp. 805–810, 2014.

[7] G. A. Zhu, L. M. Dou, and A. Y. Cao, "Assessment and analysis of strata movement with special reference to rock burst mechanism in island longwall panel," *Journal of Central South University*, vol. 24, no. 012, pp. 2951–2960, 2017.

[8] P. Kong, L. Jiang, and J. Jiang, "Numerical analysis of roadway rock-burst hazard under superposed dynamic and static loads," *Energies*, vol. 12, 2019.

[9] L. Dou, T. Chen, S. Gong, H. He, and S. Zhang, "Rockburst hazard determination by using computed tomography technology in deep workface," *Safety Science*, vol. 50, no. 4, pp. 736–740, 2012.

[10] Q. Wang, Z. Jiang, B. Jiang, H. Gao, Y. Huang, and P. Zhang, "Research on an automatic roadway formation method in deep mining areas by roof cutting with high-strength bolt-grouting," *International Journal of Rock Mechanics and Mining Sciences*, vol. 128, Article ID 104264, 2020.

[11] Q. Wang, Y. Wang, M. He et al., "Experimental research and application of automatically formed roadway without advance tunneling," *Tunnelling and Underground Space Technology*, vol. 114, no. 3, Article ID 103999, 2021.

[12] Y. Wang, W. K. Feng, R. L. Hu, and C. H. Li, "Fracture evolution and energy characteristics during marble failure under triaxial fatigue cyclic and confining pressure unloading (FC-CPU) conditions," *Rock Mechanics and Rock Engineering*, vol. 54, no. 2, pp. 799–818, 2021.

[13] X. Lai, H. Xu, J. Fan et al., "Study on the mechanism and control of rock burst of coal pillar under complex conditions," *Geofluids*, vol. 2020, no. 2, 19 pages, Article ID 8847003, 2020.

[14] S. He, D. Song, and Z. Li, "Mechanism and prevention of rockburst in steeply inclined and extremely thick coal seams for fully mechanized top-coal caving mining and under gob filling conditions," *Energies*, vol. 13, 2020.

[15] W. Guo, Y. Li, D. Yin, S. Zhang, and X. Sun, "Mechanisms of rock burst in hard and thick upper strata and rock-burst controlling technology," *Arabian Journal of Geosciences*, vol. 9, no. 10, p. 561, 2016.

[16] G. Li, Y. Hu, and Q. B. Li, "Inversion method of in-situ stress and rock damage characteristics in dam site using neural network and numerical simulation—a case study," *IEEE Access*, vol. 99, p. 1, 2020.

[17] D. Guo, X. Kang, Z. Lu, and Q. Chen, "Mechanism and control of roadway floor rock burst induced by high horizontal stress," *Shock and Vibration*, vol. 2021, no. 4, 13 pages, Article ID 6745930, 2021.

[18] J. Cao, L. Dou, G. Zhu, J. He, S. Wang, and K. Zhou, "Mechanisms of rock burst in horizontal section mining of a steeply inclined extra-thick coal seam and prevention technology," *Energies*, vol. 13, no. 22, p. 6043, 2020.

[19] Z. Liu, W. Ma, and S. Tian, "Study on the mechanical behavior of double primary support of soft rock tunnel under high ground stresses and large deformation," *Advances in Civil Engineering*, vol. 2020, no. 8, 9 pages, Article ID 8832797, 2020.

[20] X. Li, S. Chen, E. Wang, and Z. Li, "Rockburst mechanism in coal rock with structural surface and the microseismic (MS) and electromagnetic radiation (EMR) response," *Engineering Failure Analysis*, vol. 124, no. 3, Article ID 105396, 2021.

[21] F. L. He, L. Xu, and H. K. Wu, "Deviatoric stress transfer and stability of surrounding rock in large-section open-off cut roof," *Yantu Gongcheng Xuebao/Chinese Journal of Geotechnical Engineering*, vol. 36, no. 6, pp. 1122–1128, 2014.

[22] H. Kang, Y. Wu, F. Gao, J. Lin, and P. Jiang, "Fracture characteristics in rock bolts in underground coal mine roadways," *International Journal of Rock Mechanics and Mining Sciences*, vol. 62, pp. 105–112, 2013.

[23] G. Li, W. Ma, S. Tian, Z. Hongbo, F. Huabin, and W. Zou, "Groundwater inrush control and parameters optimization of curtain grouting reinforcement for the jingzhai tunnel," *Geofluids*, vol. 2021, no. 7, 10 pages, Article ID 6634513, 2021.

[24] J. Tang, S. Li, G. Qin et al., "Experiments on mechanical response and energy dissipation behavior of rockburst-prone coal samples under impact loading," *Shock and Vibration*, vol. 2021, no. 2, 10 pages, Article ID 9924456, 2021.